Discovery of novel melatonin–mydroxyquinoline hybrids as multitarget strategies for Alzheimer's disease therapy

Wei Wang[1], Tingting Pan[2], Rui Su[1], Mingbin Chen[1], Wandi Xiong[1], Congjun Xu[1]* and Ling Huang[1]*

[1]Key Laboratory of Tropical Biological Resources of Ministry of Education, School of Pharmaceutical Sciences, Hainan University, Haikou, China, [2]School of Pharmaceutical Sciences, Sun Yat-Sen University, Guangzhou, China

Alzheimer's disease (AD) is a neurodegenerative disease that seriously affects human health, and current treatment strategies are far from meeting clinical needs. Inspired by multi-target drug design strategies, a series of novel natural products-based melatonin–hydroxyquinoline hybrids were designed and synthesized, targeting anti-oxidation and metal-chelating at the same time. Most of the compounds showed significant oxygen radical absorbance capacity and $A\beta_{1-42}$ aggregation inhibition. Moreover, the compounds possess good blood-brain barrier permeability. **6b** and **6c** have a good ability to alleviate oxidative stress induced by hydrogen peroxide. **6b** and **6c** possess metal-chelating properties with the chelation ratio being 2:1. Furthermore, **6b** can significantly mitigate metal-induced $A\beta$ aggregation. This work may provide a new multi-target treatment strategy for Alzheimer's disease.

KEYWORDS

melatonin, Alzheimer's disease, natural products, multitarget strategies, hydrids

1 Introduction

Alzheimer's disease (AD) is a neurodegenerative disease characterized by memory loss and cognitive impairment, whose impact will be even more profound as the global population continues to age (Scheltens et al., 2021; Author Anonymous, 2023). The number of people affected by AD worldwide is estimated to rise from 55 million in 2020 to 135 million by 2050 (Author Anonymous, 2023). The global cost of treating AD is estimated at approximately 2.8 trillion dollars, which will create a huge social burden. The development of safe and effective anti-AD drugs has always been the hot spot in medical chemistry.

The pathogenesis of AD is complex, and many hypotheses were proposed, including the cholinergic hypothesis, the beta-amyloid cascade hypothesis, the oxidative stress hypothesis, the metal ion disorder hypothesis, etc. In the past years, major research institutions and pharmaceutical companies have invested hundreds of billions of dollars in AD. At present, the drugs that have been approved, such as AChE inhibitors and NMDAR inhibitors, only alleviate the symptoms or make them slightly better, and there is no specific drug that can completely cure AD (Cerejeira et al., 2012; Marcinkowska et al., 2021). Therefore, more and more researchers have turned their attention to the multi-target

design strategy. Multi-target drugs are expected to become a breakthrough in the treatment of AD (Rossi et al., 2021; Babaei et al., 2022; Turgutalp et al., 2022).

Melatonin (MT) is a neurohormone secreted by the pineal gland (Somalo-Barranco et al., 2022). As an endogenous natural active substance of the human body, accumulating reports suggest that melatonin has excellent antioxidant activity and a protective effect on nerve cells (He et al., 2022). Besides, MT can also chelate heavy metals, including lead, cadmium, and aluminum, while chelating iron and copper can reduce oxidative stress in the body (Reiter et al., 2016). Furthermore, clinical studies have shown that melatonin can improve cognition and mood in Alzheimer's patients (Dowling et al., 2008). In the meantime, the imbalance of metal ions in the brain will accelerate the aggregation of Aβ and Tau proteins resulting in cognitive decline. Hence, metal ion chelators, such as hydroxyquinoline derivative clioquinol (CQ) are considered potential drugs for the treatment of AD (Adlard et al., 2008; Faux et al., 2010). From this, a hypothesis can be proposed that simultaneously targeting oxidative stress and metal ion disorder may be an effective strategy for treating AD.

In this study, a series of novel melatonin–hydroxyquinoline hybrids were designed and synthesized, targeting anti-oxidation and metal ion chelation at the same time. In detail, melatonin and hydroxyquinoline were coupled by amide or amine linkage, and the connecting linker's length and the hydroxyquinoline's link location were investigated for their impact on bioactivity (Figure 1).

2 Results and discussion

2.1 Synthesis

Routes for synthesizing the target compounds (**3a-d**, **4**, **6a-d**, **11a-b** and **13a-c**) are demonstrated in Schemes 1–4. Commercially available 2-methyl-8-hydroxyquinoline (**1**) was reacted with SeO_2 in the presence of 1,4-dioxane to produce compound **2**. Dissolving different amines, compound **2** and isopropanol, they were reacted at room temperature for 3 h, then $NaBH_4$ was added and kept stirring for 12 h to obtain **3a-d**. Target compound **4** was obtained by the N-methylationst of **3a**.

The synthetic route of **6a-d** via a tow-step produce is shown in Scheme 2. Commercially available 2-methyl-8-hydroxyquinoline was reacted with SeO_2 in pyridine to produce compound **5**, followed by treatment with amines, HATU and DIPEA to mediate amine formation, so **6a-d** were obtained.

The synthesis of the target compounds **11a-b** is summarized in Scheme 3. Using $ZnCl_2$ as a catalyst, 8-hydroxyquinoline was reacted with formaldehyde and hydrochloric acid to produce **8**. Compound **8** was refluxed in DMF for 8 h. Then refluxed in hydrochloric acid for 9 h to obtain compound **10**. Followed by treatment with different substituted carboxylic acids, HATU and DIPEA to produce target **11a-b**.

As showed in Scheme 4, treatment of the commercially available 8-hydroxyquinoline-7-carboxylic acid and different amines in the presence of HATU and DIPEA afforded the target compounds **13a-b**.

2.2 Activity evaluation and structure-activity relationships

### 2.2.1 The oxygen radical absorbance capacity (ORAC)

Oxidative stress is involved in various pathological processes of AD and is one of the crucial adjective pathogeneses of AD. Therefore, it is essential to test the scavenging ability of target compounds. The oxygen radical absorbance capacity (ORAC) (Wang et al., 2014; Wang et al., 2015) was tested to evaluate the effects of compounds on oxidative stress. As shown in Table 1, MT has a satisfactory antioxidant effect, with the ORAC values of 2.38, whereas CQ had almost no antioxidant effect. Compared with the melatonin, most of the target compounds, such as 3a~3d, 4, 6a~6d, and 11a~11b, which ORAC values were greater than 2.3. while compound **13a~13c**, which is linked at position **7** of hydroxyquinoline, have weaker oxygen radical scavenging ability. This suggests that the position of the junction on CQ has a large effect on the activity. Furthermore, the change in the connecting linker's length has a slight effect on the ORAC, just as 3a and 3d have different lengths while having similar antioxidant activity.

2.2.2 Inhibition of Aβ$_{1-42}$ aggregation

Self-mediated Aβ1–42 aggregation inhibition was assessed via thioflavin T (ThT) fluorescence assay (Rosini et al., 2008; Wang et al., 2018; Babaei et al., 2022). As shown in Table 1, both CQ and MT showed good anti-aggregation effect. Most of the target compounds showed good inhibition of Aβ$_{1-42}$ aggregation. Among them, **3c**, **4**, **6a**, **6b**, **6c**, **11a**, and **13a** showed better activity than melatonin (38.96 ± 9.35) and CQ (30.76 ± 1.08). When the connection is amine, compounds with -OH substituents on the indole ring have the highest inhibitory activity against Aβ$_{1-42}$ aggregation. Compound **3c** containing hydroxyl-substituted indole ring fragments has the highest inhibitory rate against Aβ$_{1-42}$ self-aggregation (40.23%), which is much higher than the inhibition rate of methoxy-substituted and unsubstituted indole ring fragment compounds (18.23% and 27.10% respectively). When the connection mode is an amide, compound **6b** with a methoxy group on the indole ring has the highest inhibition rate (63.24%). This shows that the different substituents at position 5 on the indole ring and the different link methods between melatonin and hydroxyquinoline play an important role in inhibiting the self-aggregation of Aβ$_{1-42}$. Compared **3a** (27.10%) with **4** (52.54%), it can be found that methylation of nitrogen atoms leads to increased activity. On the whole when the connection mode is amide, the inhibitory activity is better. The length of the connected chain is shortened, and the activity decreases to different degrees. In addition, the compounds obtained at positions 2, 5 and 7 of the quinoline ring had no significant effect on the self-aggregation of Aβ$_{1-42}$ such as **6a** (45.45%), **11a** (44.74%) and **13a** (46.98%).

2.2.3 Blood−brain barrier permeability assay

The blood-brain barrier permeability of central nervous drugs is a crucial drug-like property. In this work, the parallel artificial membrane permeability assay (PAMPA) (Di et al., 2003; Wang et al., 2014) was used to evaluate the ability of compounds to cross the blood-brain barrier. 13 commercial drugs were chosen to establish the evaluation system (Supplementary Table S1). Most of the target compounds can cross the blood-brain barrier with the

FIGURE 1
The design strategy of melatonin−hydroxyquinoline hybrids.
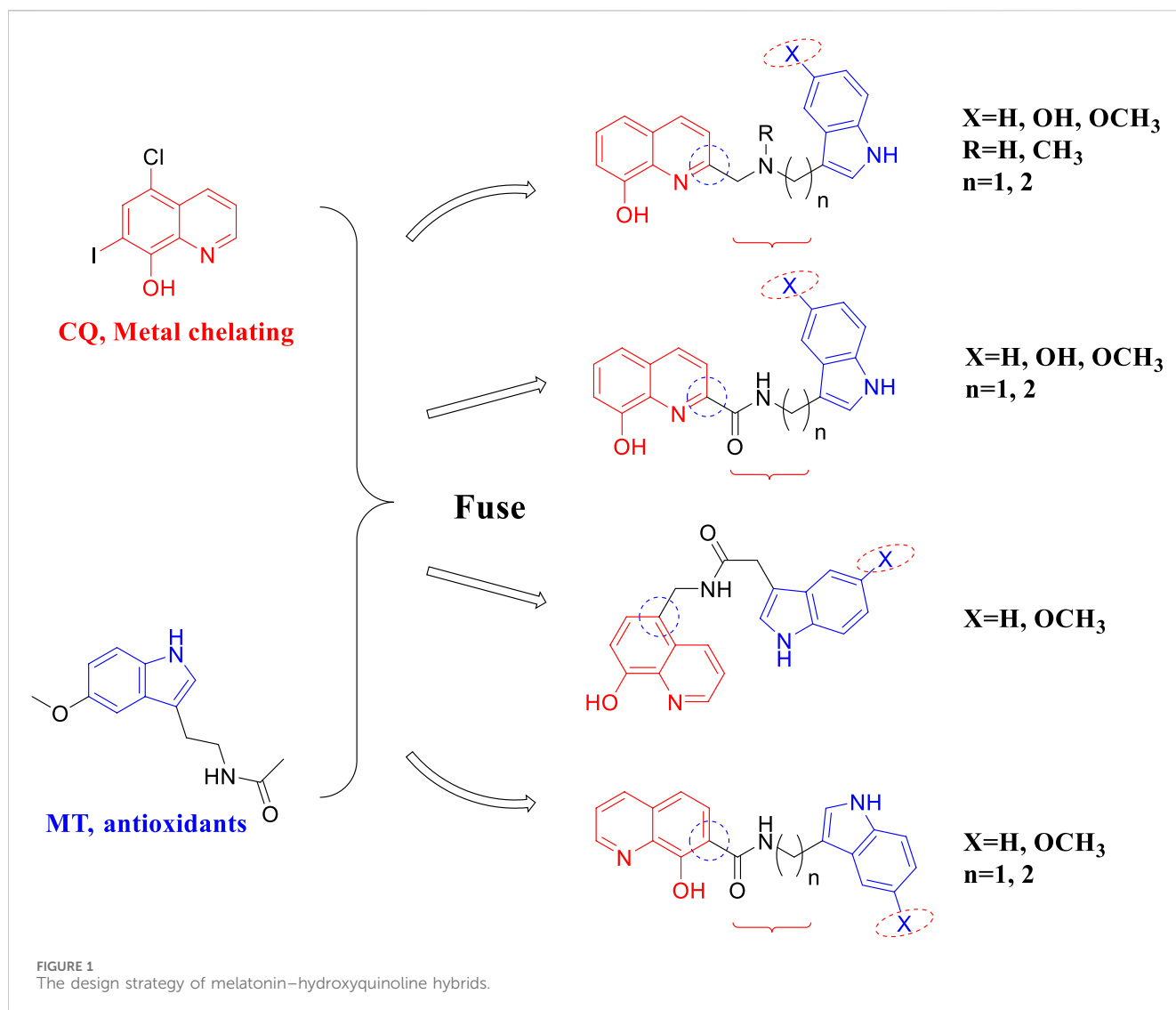
$P_e > 4.7$, such as **3a**, **3b**, **3c**, **3d**, **4**, **6a**, **6b** and **6d**. The compounds with hydroxyl groups exhibit poor BBB permeability, possibly due to increased hydrophilia.

2.2.4 Cytotoxicity assay

To further investigate the bioactivity of the compounds, cytotoxicity was evaluated on SH-SY5Y and BV2 cell lines (Figures 2A, B). The results showed that **6b** and **6c** exhibit no cytotoxicity at 5 μM in SH-SY5H cell lines while showing slight toxicity at concentrations of 10 μM. As for BV2 cells, **6b** and **6c** also showed no significant cytotoxicity at 20 μM concentration.

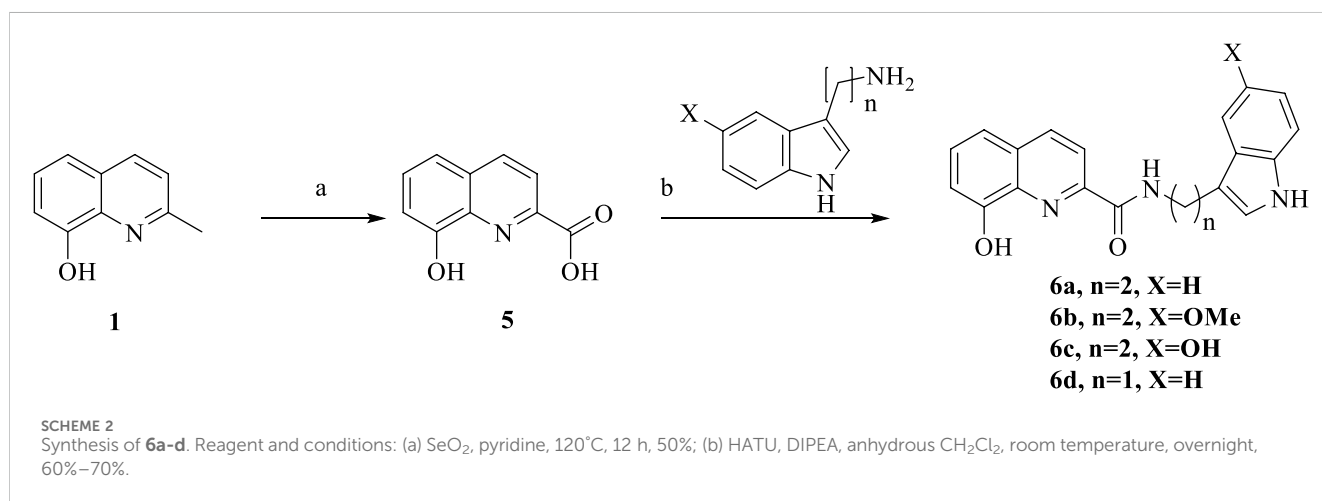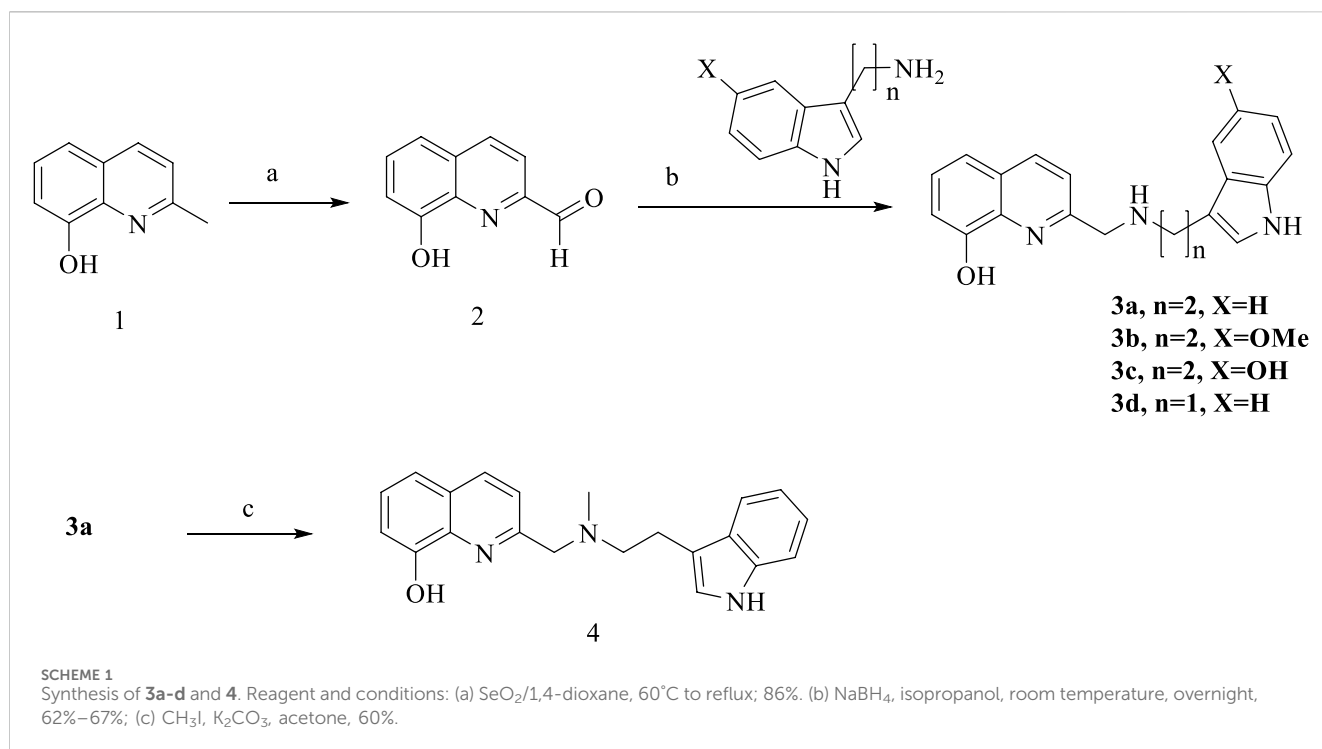## 2.2.5 Alleviating oxidative stress induced by hydrogen peroxide

The effect of **6b** and **6c** on the oxidative stress of SH-SY5H cells induced by hydrogen peroxide was investigated using DCFH-DA as the fluorescent probe (Xu et al., 2021). The results showed that the ROS increased sharply in SH-SY5H cells treated with 400 μM hydrogen peroxide for 12 h. Pretreatment with **6b** or **6c** reduced ROS production in a dose-dependent manner, suggesting that **6b** and **6c** have a good ability to alleviate oxidative stress (Figure 2C).

2.2.6 Metal-chelating property

To further evaluate multi-target anti-AD potential, the metal-chelating properties of **6b** and **6c** were determined by UV spectrophotometry (Geng et al., 2012; Lu et al., 2013; Hu et al., 2019). As shown in Figures 3A, C, **6b** exhibited a maximum absorption peak at 255 nm, and the maximum absorption peak showed a significant redshift and the intensity decreased when **6b** co-incubated with Cu^{2+} or Zn^{2+}. While co-incubated with Fe^{3+} or Fe^{2+}, the intensity at 255 nm was in different degrees decreased. The same result occurred for **6c**. Those results suggested that **6b** and **6c** possess metal-chelating properties. Next, the chelation ratios of **6b** and **6c** to Cu^{2+} were measured and calculated using the inflection point method (Figures 3B, D). The inflection point appears when the concentration ratio of compound Cu^{2+} to **6b** or **6c** is 0.5, so it can be inferred that the chelation ratio of compound **6b** and **6c** to Cu^{2+} is 2:1.

2.2.7 Effect of Cu^{2+}-induced Aβ aggregation

To further detect the ability of compounds **6b**, CQ and MT to disaggregate or inhibit the Cu^{2+}-induced $Aβ_{1-42}$ aggregation, we conducted thioflavin T fluorometric detection (Hu et al., 2019). The results showed that compounds **6b** and CQ both significantly

SCHEME 1
Synthesis of **3a-d** and **4**. Reagent and conditions: (a) SeO$_2$/1,4-dioxane, 60°C to reflux; 86%. (b) NaBH$_4$, isopropanol, room temperature, overnight, 62%–67%; (c) CH$_3$I, K$_2$CO$_3$, acetone, 60%.

SCHEME 2
Synthesis of **6a-d**. Reagent and conditions: (a) SeO$_2$, pyridine, 120°C, 12 h, 50%; (b) HATU, DIPEA, anhydrous CH$_2$Cl$_2$, room temperature, overnight, 60%–70%.

disaggregated Cu^{2+}-induced Aβ$_{1-42}$ aggregation, also with the mild disaggregated effect of MT (Figure 4A). As shown in Figure 4B, **6b** exhibited a distinct inhibitory effect on Cu^{2+}-induced Aβ$_{1-42}$ aggregation, which was superior to the reference compound CQ, while MT exhibited weak inhibitory activity. Those results suggest that **6b** can significantly mitigate metal ion induced Aβ aggregation.
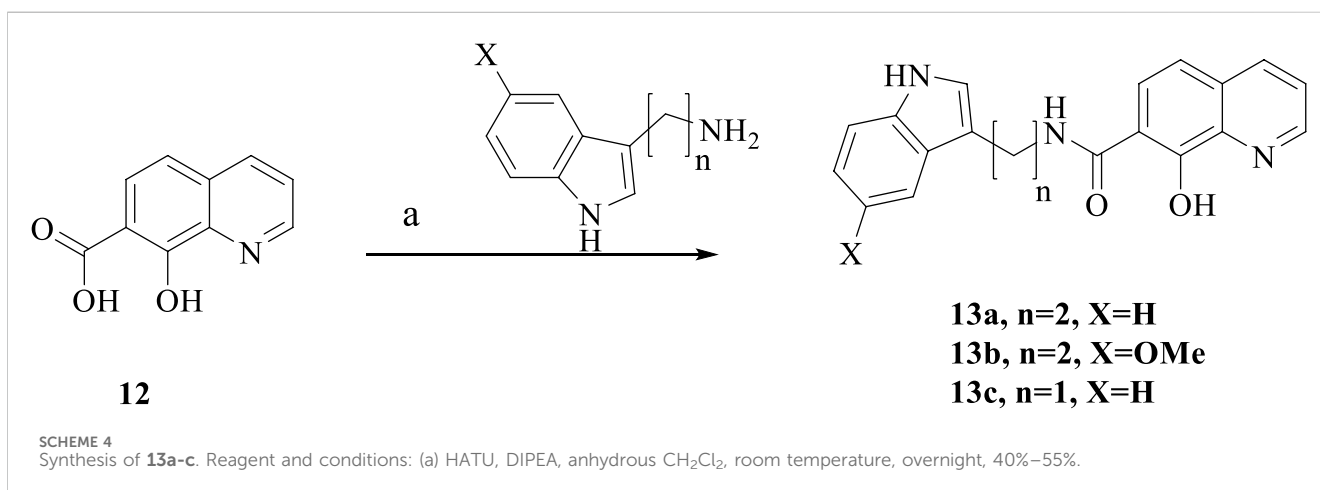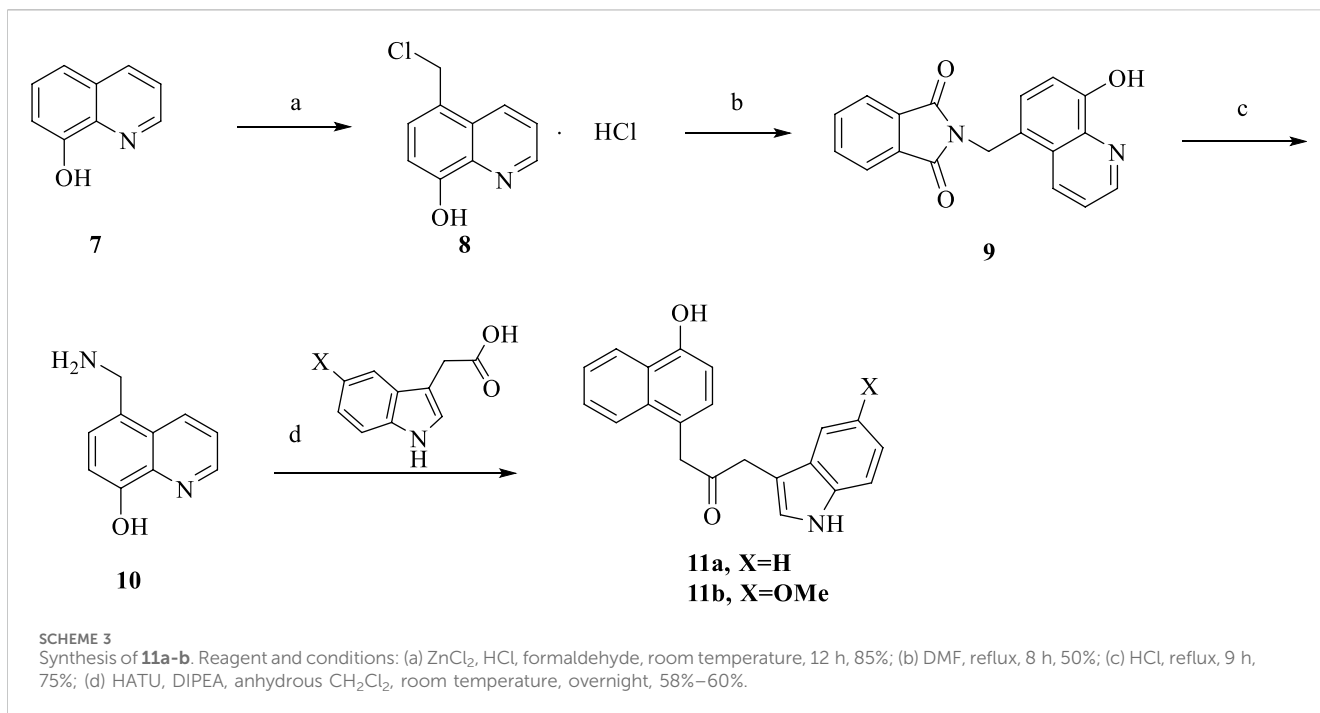
3 Experimental

3.1 Chemistry

3.1.1 8-hydroxyquinoline-2-carbaldehyde (**2**)

At 60°C, 10 mL dioxane solution of 2-methyl-8-hydroxyquinoline (10 mmol) was added to 50 mL dioxane

solution of SeO$_2$ (20 mmol). After half an hour of drip adding, the reaction reflux for 4 h. Yield 86%. ^{1}H NMR (400 MHz, Acetone-d_6) δ 10.16 (s, 1H), 9.22 (s, 1H), 8.55 (d, J = 8.5 Hz, 1H), 8.04 (d, J = 8.5 Hz, 1H), 7.69 (t, J = 8.0 Hz, 1H), 7.57 (dd, J = 8.2, 0.9 Hz, 1H), 7.28 (dd, J = 7.7, 1.0 Hz, 1H).

3.1.2 8-hydroxyquinoline-2-carboxylic acid (5)

1 (20 mmol) was dissolved in pyridine (50 mL), and SeO$_2$ (20 mmol) was added followed by stirring at 120°C for 12 h, after the completion of the reaction (monitored by TLC). The reaction mixture was filtered off first. The solvent was distilled off and the residue was dissolved in an aqueous KOH solution (10%), Then filtered and the filtered liquid was acidified with hydrochloric acid (10%). Last the filtered crude product was purified by silica-column chromatography. yellow solid, yield 50%.^{1}H NMR (400 MHz,

SCHEME 3
Synthesis of **11a-b**. Reagent and conditions: (a) ZnCl$_2$, HCl, formaldehyde, room temperature, 12 h, 85%; (b) DMF, reflux, 8 h, 50%; (c) HCl, reflux, 9 h, 75%; (d) HATU, DIPEA, anhydrous CH$_2$Cl$_2$, room temperature, overnight, 58%–60%.

SCHEME 4
Synthesis of **13a-c**. Reagent and conditions: (a) HATU, DIPEA, anhydrous CH$_2$Cl$_2$, room temperature, overnight, 40%–55%.

Acetone-d_6) δ 9.68 (s, 1H), 8.63 (d, J = 8.5 Hz, 1H), 8.27 (d, J = 8.5 Hz, 1H), 7.70 (t, J = 7.9 Hz, 1H), 7.60 (d, J = 8.2 Hz, 1H), 7.28 (d, J = 7.6 Hz, 1H).

3.1.3 5-(Chloromethyl)quinolin-8-ol hydrochloride (8·HCl)

Compound **8** was synthesized according to the literature. Pale yellow solid, yield 98%. ^{1}H NMR (400 MHz, DMSO-d_6) δ 9.22 (d, J = 7.9 Hz, 1H), 9.13 (dd, J = 5.0, 1.1 Hz, 1H), 8.12 (dd, J = 8.6, 5.1 Hz, 1H), 7.87 (d, J = 8.0 Hz, 1H), 7.51 (d, J = 8.0 Hz, 1H), 5.33 (s, 2H).
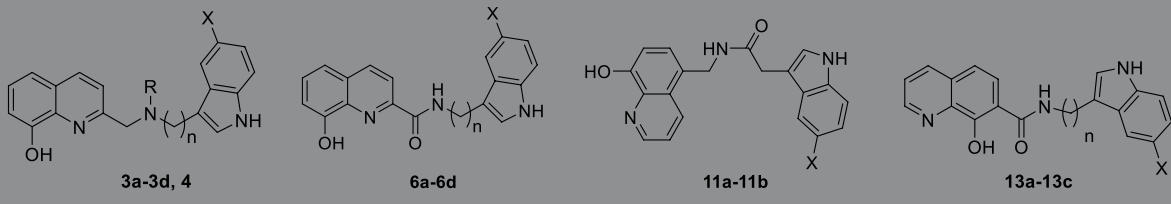
3.1.4 2-(hydroxyquinoline-5-yl-methyl)-isoquino line-1,3-diketone (9)

Under the nitrogen atmosphere. A mixture of phthalimide potassium (4.5 mmol), 5-(Chloromethyl)quinolin-8-ol Hydrochloride (3 mmol) and DMF (10 mL) was heated to 150°C, and refluxed for 8 h. After cooling to room temperature, the white

potassium chloride residue was formed at the bottom of the flask, which was filtered. The filtrate was poured into water (400 mL), and filtered to obtain compound **9**. White solid, yields 73%. ^{1}H NMR (400 MHz, DMSO-d_6) δ 9.82 (s, 1H), 8.88 (dd, J = 4.1, 1.2 Hz, 1H), 8.73 (dd, J = 8.6, 1.3 Hz, 1H), 7.92–7.87 (m, 2H), 7.87–7.82 (m, 2H), 7.65 (dd, J = 8.6, 4.1 Hz, 1H), 7.45 (d, J = 7.9 Hz, 1H), 7.03 (d, J = 7.9 Hz, 1H), 5.14 (s, 2H).

3.1.5 5-aminomethyl-8-hydroxyquinoline (10)

To a stirred concentrated hydrochloric acid (20 mL), compound **9** (2.19 mmol) was added, refluxed for 9 h until the mixture became transparent after cooling to room temperature. The solvent was distilled off and the residue was dissolved in water, then the solution pH to produce a solid. Greenish solid, yield 75%. ^{1}H NMR (400 MHz, DMSO-d_6) δ 8.85 (dd, J = 4.1, 1.4 Hz, 1H), 8.56 (dd, J = 8.5, 1.4 Hz, 1H), 7.57 (dd, J = 8.5, 4.1 Hz, 1H), 7.42 (d, J = 7.8 Hz, 1H), 7.01 (d, J = 7.8 Hz, 1H), 4.08 (s, 2H).

TABLE 1 Oxygen radical absorbance capacity, PAMPA assay and inhibition of $A\beta_{1-42}$ self-aggregation for target compounds.

Compound	n	X	R	ORAC[a]	Inhibition of $A\beta_{1-42}$ aggregation (%)[b]	P_e (× 10^{-6} cm s^{-1})[c]	pred
3a	2	H	H	3.50 ± 0.12	27.10 ± 5.01	8.08 ± 0.56	CNS+
3b	2	OMe	H	3.25 ± 0.10	18.23 ± 2.02	6.61 ± 0.22	CNS+
3c	2	OH	H	4.47 ± 0.18	40.23 ± 2.89	4.81 ± 0.87	CNS+
3d	1	H	H	2.60 ± 0.20	20.47 ± 4.72	5.09 ± 1.32	CNS+
4	2	H	Me	2.93 ± 0.15	52.54 ± 6.47	9.87 ± 0.66	CNS+
6a	2	H	—	2.49 ± 0.22	45.45 ± 0.41	7.71 ± 0.61	CNS+
6b	2	OMe	—	2.76 ± 0.01	63.24 ± 2.02	6.91 ± 0.92	CNS+
6c	2	OH	—	3.23 ± 0.02	40.33 ± 2.09	2.96 ± 0.58	CNS±
6d	1	H	—	2.32 ± 0.17	19.25 ± 5.85	6.81 ± 1.13	CNS+
11a	2	H	—	2.91 ± 0.16	44.74 ± 5.18	2.82 ± 0.42	CNS±
11b	2	OMe	—	3.58 ± 0.12	34.94 ± 2.91	1.35 ± 0.25	CNS−
13a	2	H	—	1.06 ± 0.07	46.98 ± 6.25	3.98 ± 0.45	CNS±
13b	2	OMe	—	1.33 ± 0.02	19.66 ± 2.06	1.12 ± 0.42	CNS−
13c	1	H	—	0.94 ± 0.02	38.58 ± 5.12	2.65 ± 0.46	CNS±
CQ	—	—		0.54 ± 0.17	30.76 ± 1.08	NT	NT
Melatonin	—	—		2.38 ± 0.12	38.96 ± 9.35	NT	NT
Curcumin	—	—		NT	52.88 ± 6.38	NT	NT
Chlorpromazinne	—	—		NT	NT	6.63 ± 0.81	CNS+
Hydrocortisone	—	—		NT	NT	1.13 ± 0.15	CNS−

[a]Result is the mean of three independent experiments (n = 3) ± SD.
[b]Result are the mean of three independent experiments (n = 3) ± SD., The concentration of all compounds was 20 μM.
[c]Result are the mean of three independent experiments (n = 3) ± SD., Compounds could potentially cross the BBB, when Pe > 4.7 × 10−6 cm s−1.
NT, not tested.

3.1.5.1 General method for the preparation of compounds 3a–3d

To a solution of **2** (1 mmol) and different indole (1 mmol) in isopropyl alcohol. After stirring at room temperature for 3 h, the $NaBH_4$ (2 mmol) was added and kept stirring for 12 h. Quenched with water, extracted with ethyl acetate, the organic layer was dried with Na_2SO_4 and concentrated under reduced pressure. The residue was purified by silica gel chromatography to afford **3a-3d** (CH_2Cl_2/ CH_3OH = 50:1).
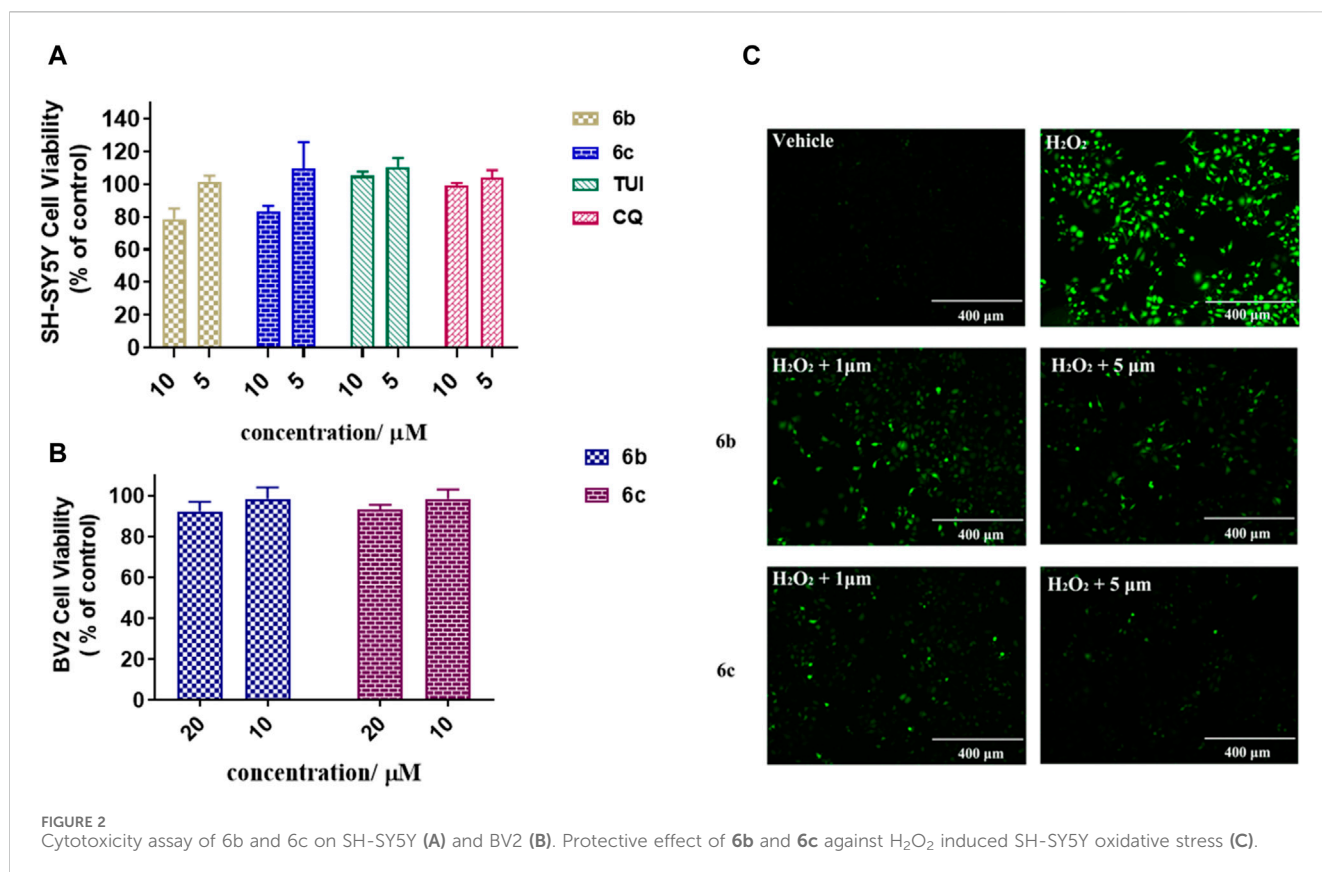
3.1.6 2-(((2-(1H-indol-3-yl)ethyl)amino)methyl)quinolin-8-ol (3a)

Yellow solid, yield 65%. ^{1}H NMR (400 MHz, DMSO-d_6) δ 10.76 (s, 1H), 8.24 (d, J = 8.5 Hz, 1H), 7.56 (d, J = 8.5 Hz, 1H), 7.51 (d, J = 7.8 Hz, 1H), 7.42–7.37 (m, 1H), 7.37–7.33 (m, 1H), 7.32 (d, J = 8.1 Hz, 1H), 7.14 (d, J = 1.8 Hz, 1H), 7.09–7.06 (m, 1H), 7.06–7.01 (m, 1H), 6.94 (t, J = 7.4 Hz, 1H), 4.07 (s, 2H), 2.91 (s, 2H), 2.90

(s, 2H). ^{13}C NMR (126 MHz, DMSO-d_6) δ 159.23, 153.23, 137.91, 136.69, 136.66, 128.05, 127.75, 127.23, 122.96, 121.45, 121.28, 118.76, 118.58, 117.98, 113.10, 111.79, 111.46, 55.13, 50.53, 26.04. HRMS (ESI) m/z calcd for $C_{20}H_{19}N_3O$ [M + H]$^+$, 318.1562; found, 318.1562. HPLC purity: 99.6%, retention time: 8.8 min.

3.1.7 2-(((2-(5-methoxy-1H-indol-3-yl)ethyl)amino)methyl)quinolin-8-ol (3b)

Yellow solid, yield 67%. ^{1}H NMR (400 MHz, DMSO-d_6) δ 10.61 (s, 1H), 8.25 (d, J = 8.5 Hz, 1H), 7.57 (d, J = 8.5 Hz, 1H), 7.42–7.37 (m, 1H), 7.37–7.31 (m, 1H), 7.20 (d, J = 8.7 Hz, 1H), 7.10 (d, J = 2.1 Hz, 1H), 7.07 (dd, J = 7.0, 1.6 Hz, 1H), 6.94 (d, J = 2.2 Hz, 1H), 6.68 (dd, J = 8.7, 2.3 Hz, 1H), 4.08 (s, 2H), 3.68 (s, 3H), 2.88 (s, 4H). ^{13}C NMR (126 MHz, DMSO-d_6) δ 159.19, 153.34, 153.24, 137.91, 136.66, 131.83, 128.05, 128.01, 127.24, 123.67, 121.45, 117.97, 112.85, 112.45, 111.48, 111.46, 100.47, 55.70, 55.06, 50.38, 26.05. HRMS (ESI) m/z calcd for $C_{21}H_{21}N_3O_2$

FIGURE 2
Cytotoxicity assay of 6b and 6c on SH-SY5Y **(A)** and BV2 **(B)**. Protective effect of **6b** and **6c** against H_2O_2 induced SH-SY5Y oxidative stress **(C)**.

$[M + H]^+$, 348.1678; found,348.1667. HPLC purity: 98.6%. Retention time: 8.7 min.

3.1.8 2-(((2-(5-hydroxy-1H-indol-3-yl)ethyl)amino) methyl)quinolin-8-ol (3c)

Yellow solid, yield 62%. ^{1}H NMR (400 MHz, DMSO-d_6) δ 10.45 (s, 1H), 8.26 (d, J = 8.5 Hz, 1H), 7.57 (d, J = 8.5 Hz, 1H), 7.45–7.38 (m, 1H), 7.38–7.33 (m, 1H), 7.12 (d, J = 8.6 Hz, 1H), 7.08 (dd, J = 7.0, 1.4 Hz, 1H), 7.04 (d, J = 1.7 Hz, 1H), 6.83 (d, J = 1.9 Hz, 1H), 6.58 (dd, J = 8.6, 2.1 Hz, 1H), 4.10 (s, 2H), 3.00 (d, J = 6.8 Hz, s), 2.85 (d, J = 6.6 Hz, 2H). ^{13}C NMR (126 MHz, DMSO-d_6) δ 158.84, 153.22, 150.59, 137.88, 136.73, 131.29, 128.42, 128.06, 127.29, 123.46, 121.40, 118.00, 112.11, 111.96, 111.68, 111.51, 102.73, 55.01, 50.37, 26.01. HRMS (ESI) m/z calcd for $C_{20}H_{19}N_3O_2$ $[M + H]^+$, 348.1678; found,348.1667. HPLC purity: 98.1%. Retention time: 8.4 min.

3.1.9 2-((((1H-indol-3-yl)methyl)amino)methyl) quinolin-8-ol (3d)

Yellow solid, yield 64%. ^{1}H NMR (400 MHz, DMSO-d_6) δ 10.90 (s, 1H), 8.25 (d, J = 8.5 Hz, 1H), 7.65 (d, J = 7.8 Hz, 1H), 7.58 (d, J = 8.5 Hz, 1H), 7.41–7.38 (m, 1H), 7.38–7.36 (m, 1H), 7.36–7.34 (m, 1H), 7.30 (s, 1H), 7.10–7.08 (m, 1H), 7.08–7.06 (m, 1H), 6.97 (t, J = 7.2 Hz, 1H), 4.07 (s, 2H), 3.99 (s, 2H). ^{13}C NMR (126 MHz, DMSO-d_6) δ 158.77, 153.24, 137.89, 136.82, 136.68, 128.06, 127.52, 127.26, 124.32, 121.49, 121.43, 119.34, 118.79, 117.98, 113.49, 111.80, 111.50, 54.35, 44.43. HRMS (ESI) m/z calcd for $C_{19}H_{17}N_3O$ $[M + H]^+$, 304.1423; found,304.1405. HPLC purity: 98. Retention time: 13.7 min.

3.1.10 2-(((2-(1H-indol-3-yl)ethyl)(methyl)amino) methyl)quinolin-8-ol (4)

To a solution of **3a** (0.5 mmol) and K_2CO_3 (1 mmol) in acetone, CH_3I (0.5 mmol) was added slowly. After being stirred at room temperature overnight, the solvent was evaporated, followed by extraction with CH_2Cl_2. The combined organic layer was dried over anhydrous Na_2SO_4 and concentrated under reduced pressure. The residue was purified by silica gel chromatography to afford yellow oil (CH_2Cl_2/CH_3OH = 30: 1). Yellow solid, yield 66%. ^{1}H NMR (400 MHz, MeOD) δ 8.16 (d, J = 8.5 Hz, 1H), 7.44 (d, J = 8.4 Hz, 1H), 7.41 (s, 1H), 7.39 (s, 1H), 7.33 (d, J = 7.6 Hz, 1H), 7.29 (d, J = 8.1 Hz, 1H), 7.10 (d, J = 7.5 Hz, 1H), 7.04 (d, J = 7.6 Hz, 1H), 7.02 (s, 1H), 6.88 (t, J = 7.5 Hz, 1H), 4.00 (s, 2H), 3.06 (dd, J = 9.8, 6.4 Hz, 2H), 2.87 (dd, J = 9.7, 6.4 Hz, 2H), 2.50 (s, 3H).^{13}C NMR (126 MHz, MeOD) δ 156.15, 153.00, 138.01, 136.73, 136.46, 128.00, 127.22, 127.04, 121.74, 121.40, 120.87, 118.10, 117.80, 117.40, 112.18, 110.83, 110.66, 62.75, 58.27, 41.63, 22.31. HRMS (ESI) m/z calcd for $C_{21}H_{21}N_3O$ $[M + H]^+$, 332.1732; found, 332.1718. HPLC purity: 97.8%. Retention time: 11.6 min.

3.1.10.1 General method for the preparation of compounds 6a-6d, 11a-11b and 13a-13c

To a solution of quinoline acid or quinoline amine (1 mmol) and indole amine or indole acid (1.3 mmol) in anhydrous CH_2Cl_2, HATU (1 mmol) and DIPEA (2 mmol) were added. After stirred at room temperature overnight, the reaction was extracted with CH_2Cl_2. The combined organic phase was dried and evaporated, the target compounds were purified by column chromatography *via* CH_2Cl_2/MeOH mixture. (CH_2Cl_2: MeOH = 50:1.)
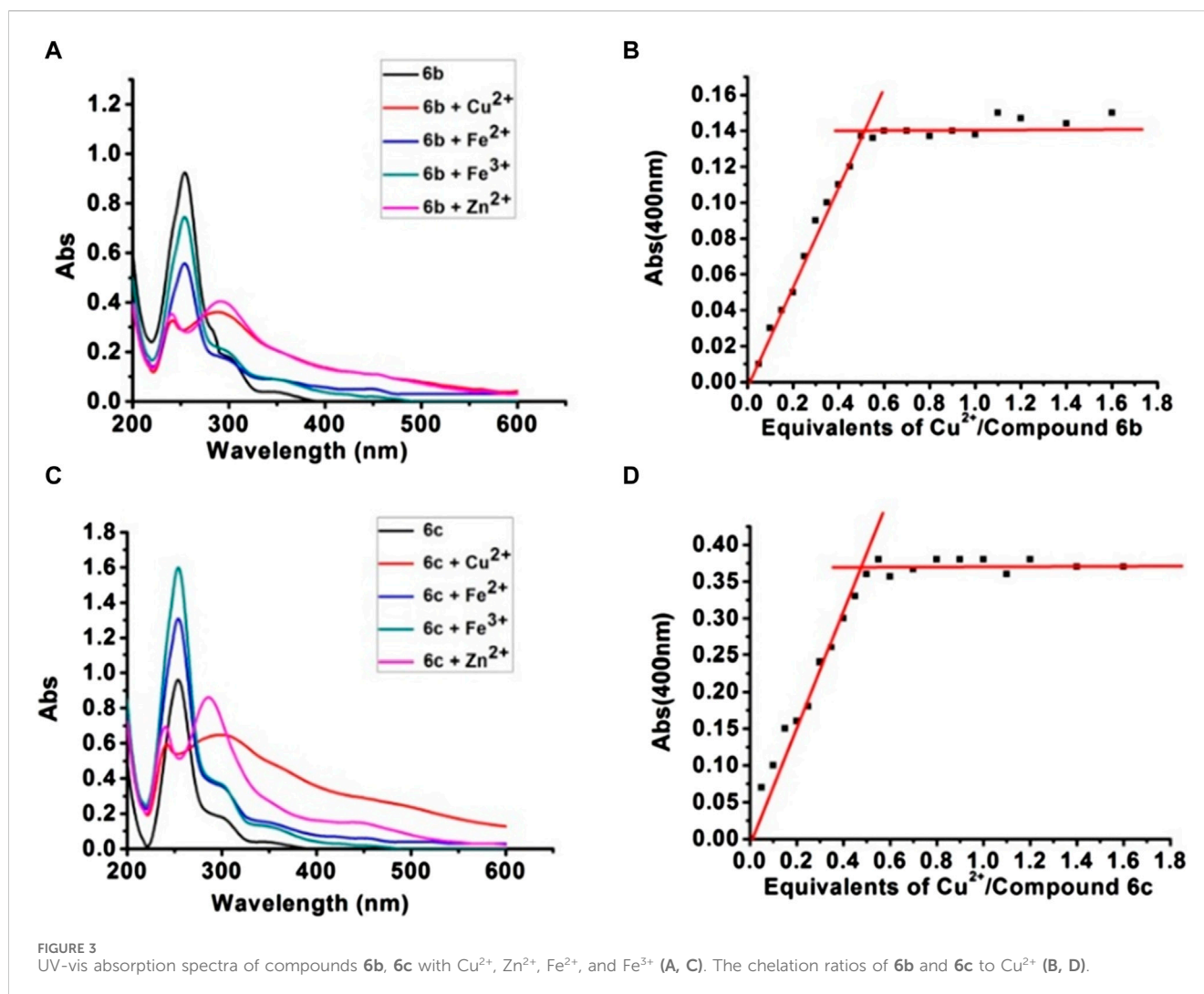
FIGURE 3
UV-vis absorption spectra of compounds **6b**, **6c** with Cu^{2+}, Zn^{2+}, Fe^{2+}, and Fe^{3+} **(A, C)**. The chelation ratios of **6b** and **6c** to Cu^{2+} **(B, D)**.

3.1.11 N-(2-(1H-indol-3-yl) ethyl)-8-hydroxyquinoline-2-carboxamide (6a)

Pale yellow solid, yield 60%. ^{1}H NMR (500 MHz, DMSO-d_6) δ 10.85 (s, 1H), 10.13 (s, 1H), 9.82 (t, J = 6.0 Hz, 1H), 8.51 (d, J = 8.5 Hz, 1H), 8.17 (d, J = 8.5 Hz, 1H), 7.63 (d, J = 7.8 Hz, 1H), 7.57 (t, J = 7.9 Hz, 1H), 7.52–7.45 (m, 1H), 7.35 (d, J = 8.1 Hz, 1H), 7.22 (d, J = 2.1 Hz, 1H), 7.18 (dd, J = 7.6, 0.9 Hz, 1H), 7.07 (t, J = 7.5 Hz, 1H), 6.99 (t, J = 7.4 Hz, 1H), 3.69 (dd, J = 14.7, 6.6 Hz, 2H), 3.05 (t, J = 7.6 Hz, 2H). ^{13}C NMR (126 MHz, DMSO-d_6) δ 164.11, 154.08, 148.09, 138.19, 136.88, 136.72, 129.92, 129.81, 127.70, 123.15, 121.44, 119.29, 118.75, 118.64, 118.01, 112.22, 111.99, 111.89, 25.90. HRMS (ESI) m/z calcd for $C_{20}H_{17}N_3O_2$ [M + H]$^+$, 332.1732; found,332.1354. HPLC purity: 98.3%. Retention time: 15.4 min.
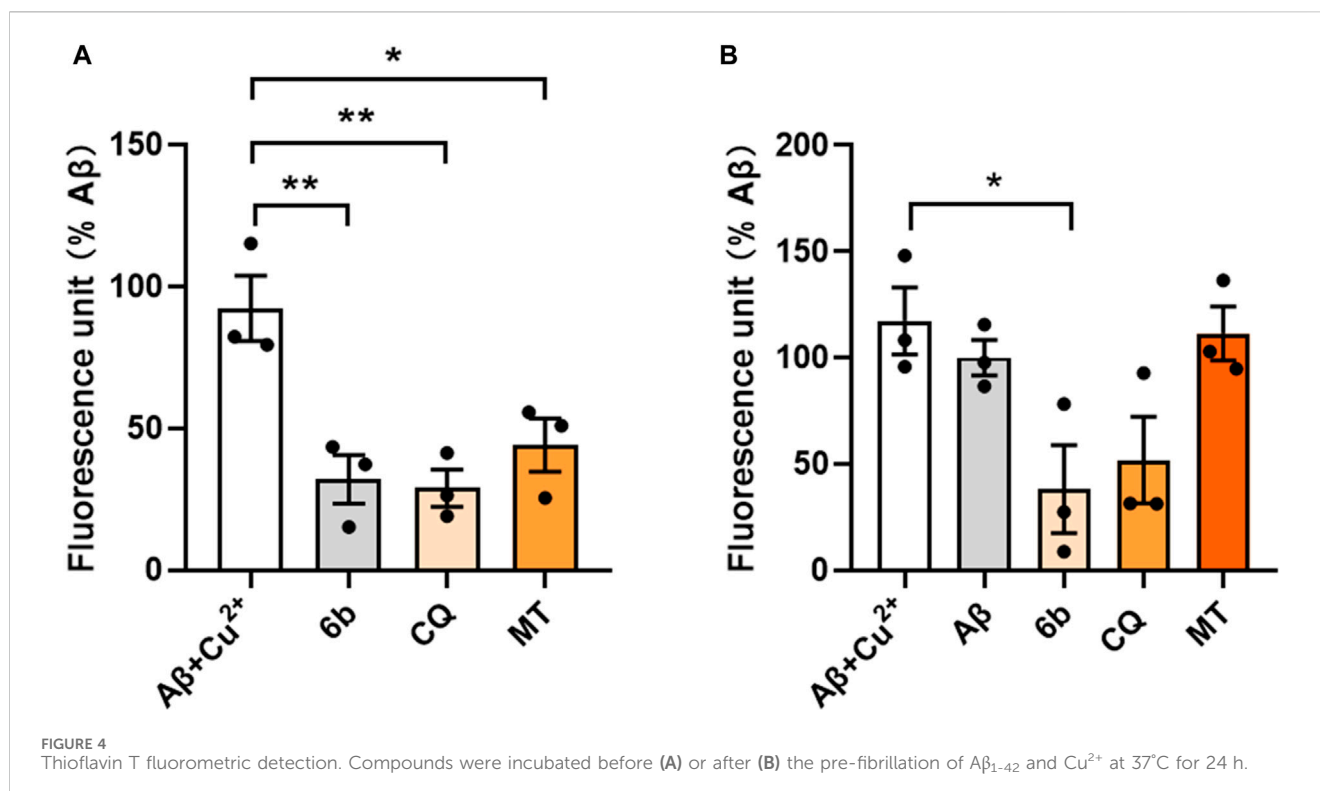
3.1.12 8-hydroxy-N-(2-(5-methoxy-1H-indol-3-yl)ethyl)quinoline-2-carboxamide (6b)

Pale yellow solid, yield 62%. ^{1}H NMR (500 MHz, DMSO-d_6) δ 10.69 (s, 1H), 10.15 (s, 1H), 9.83 (s, 1H), 8.50 (d, J = 8.3 Hz, 1H), 8.19 (d, J = 8.3 Hz, 1H), 7.57 (t, J = 7.6 Hz, 1H), 7.49 (d, J = 7.8 Hz, 1H), 7.25 (d, J = 8.5 Hz, 1H), 7.20 (s, 1H), 7.18 (s, 1H), 7.12 (s, 1H), 6.72

(d, J = 8.0 Hz, 1H), 3.72 (s, 3H), 3.69 (s, 2H), 3.04 (s, 2H). ^{13}C NMR (126 MHz, DMSO-d_6) δ 164.12, 154.08, 153.48, 148.11, 138.17, 136.89, 131.84, 129.91, 129.81, 128.05, 123.83, 119.29, 118.00, 112.52, 112.12, 111.99, 111.63, 100.56, 55.71, 25.90. HRMS (ESI) m/z calcd for $C_{21}H_{19}N_3O_3$ [M + H]$^+$, 362.1471; found, 362.1460. HPLC purity: 99.6%. Retention time: 13.4 min.

3.1.13 8-hydroxy-N-(2-(5-hydroxy-1H-indol-3-yl)ethyl)quinoline-2-carboxamide (6c)

Pale yellow solid, yield 60%. ^{1}H NMR (400 MHz, DMSO-d_6) δ 10.50 (s, 1H), 10.11 (s, 1H), 9.78 (t, J = 5.8 Hz, 1H), 8.60 (s, 1H), 8.51 (d, J = 8.5 Hz, 1H), 8.18 (d, J = 8.5 Hz, 1H), 7.57 (t, J = 7.9 Hz, 1H), 7.49 (d, J = 8.0 Hz, 1H), 7.18 (d, J = 7.5 Hz, 1H), 7.14 (d, J = 8.6 Hz, 1H), 7.11 (d, J = 1.8 Hz, 1H), 6.93 (d, J = 1.9 Hz, 1H), 6.61 (dd, J = 8.6, 2.1 Hz, 1H), 3.65 (dd, J = 14.8, 6.6 Hz, 2H), 2.99–2.93 (m, 2H). ^{13}C NMR (126 MHz, DMSO-d_6) δ 164.09, 154.07, 150.72, 148.12, 138.18, 136.89, 131.30, 129.92, 129.81, 128.37, 123.57, 119.29, 118.01, 112.18, 111.99, 111.82, 111.24, 102.70, 26.03. HRMS (ESI) m/z calcd for $C_{20}H_{17}N_3O_3$ [M + H]$^+$, 348.1313; found, 348.1303. HPLC purity: 99.5%. Retention time: 8.0 min.

FIGURE 4
Thioflavin T fluorometric detection. Compounds were incubated before **(A)** or after **(B)** the pre-fibrillation of Aβ$_{1-42}$ and Cu^{2+} at 37°C for 24 h.

3.1.14 N-((1H-indol-3-yl)methyl)-8 -hydroxyquino line-2-carboxamide (6d)

Pink solid, yield 60%. ^{1}H NMR (400 MHz, DMSO-d_6) δ 10.96 (s, 1H), 10.14 (s, 1H), 9.89 (t, J = 5.9 Hz, 1H), 8.50 (d, J = 8.6 Hz, 1H), 8.23 (t, J = 8.3 Hz, 1H), 7.65 (d, J = 7.9 Hz, 1H), 7.54 (t, J = 7.9 Hz, 1H), 7.46 (d, J = 8.1 Hz, 1H), 7.39–7.37 (m, 1H), 7.37–7.35 (m, 1H), 7.13 (d, J = 7.5 Hz, 1H), 7.07 (t, J = 7.5 Hz, 1H), 6.97 (t, J = 7.5 Hz, 1H), 4.77 (d, J = 5.9 Hz, 2H). ^{13}C NMR (126 MHz, DMSO-d_6) δ 163.90, 154.13, 148.13, 138.16, 136.91, 136.87, 129.91, 129.80, 126.96, 124.49, 121.67, 119.47, 119.23, 119.07, 117.96, 112.77, 112.01, 111.98, 34.80. HRMS (ESI) m/z calcd for C$_{19}$H$_{15}$N$_3$O$_2$ [M + H]$^+$, 318.1573; found, 318.1198. HPLC purity: 97.9%. Retention time: 16.5 min.

3.1.15 N-((8-hydroxyquinolin-5-yl)methyl)-2-(1H-indol-3-yl)acetamide (11a)

Pale white solid, yield 58%. ^{1}H NMR (400 MHz, DMSO-d_6) δ 10.83 (s, 1H), 9.72 (s, 1H), 8.85 (d, J = 3.8 Hz, 1H), 8.43 (d, J = 8.6 Hz, 1H), 8.35 (t, J = 5.1 Hz, 1H), 7.53–7.48 (m, 1H), 7.48–7.43 (m, 1H), 7.37 (d, J = 7.8 Hz, 1H), 7.32 (d, J = 8.1 Hz, 1H), 7.15 (s, 1H), 7.05 (t, J = 7.5 Hz, 1H), 6.99 (d, J = 7.7 Hz, 1H), 6.90 (t, J = 7.4 Hz, 1H), 4.62 (d, J = 5.5 Hz, 2H), 3.54 (s, 2H). ^{13}C NMR (126 MHz, DMSO-d_6) δ 170.93, 153.21, 148.24, 139.12, 136.56, 133.23, 128.21, 127.66, 127.30, 125.53, 124.24, 122.14, 121.38, 119.19, 118.65, 111.74, 110.66, 109.32, 54.05, 33.16. HRMS (ESI) m/z calcd for C$_{20}$H$_{17}$N$_3$O$_2$ [M + H]$^+$, 332.1364; found, 332.1354. HPLC purity: 95.2%. Retention time: 8.2 min.

3.1.16 N-((8-hydroxyquinolin-5-yl)methyl)-2-(5-methoxy-1H-indol-3-yl)acetamide (11b)

Pale white solid, yield 60%. ^{1}H NMR (400 MHz, DMSO-d_6) δ 10.68 (s, 1H), 9.71 (s, 1H), 8.84 (dd, J = 4.0, 1.3 Hz, 1H), 8.42

(dd, J = 8.5, 1.2 Hz, 1H), 8.35 (t, J = 5.3 Hz, 1H), 7.47 (dd, J = 8.6, 4.1 Hz, 1H), 7.38 (d, J = 7.8 Hz, 1H), 7.22 (d, J = 8.7 Hz, 1H), 7.12 (d, J = 2.1 Hz, 1H), 6.99 (d, J = 5.7 Hz, 1H), 6.98 (s, 1H), 6.70 (dd, J = 8.7, 2.4 Hz, 1H), 4.63 (d, J = 5.6 Hz, 2H), 3.62 (s, 3H), 3.51 (s, 2H). ^{13}C NMR (126 MHz, MeOD) δ 173.08, 153.64, 152.64, 147.53, 138.78, 132.55, 131.89, 127.87, 127.29, 127.08, 124.42, 124.33, 121.35, 111.63, 111.50, 109.58, 107.81, 99.89, 54.63, 40.20, 32.85. HRMS (ESI) m/z calcd for C$_{21}$H$_{19}$N$_3$O$_3$ [M + H]$^+$, 362.1469; found, 362.1460. HPLC purity: 96.2%. Retention time: 7.5 min.

3.1.17 N-(2-(1H-indol-3-yl)ethyl)-8 -hydroxyquin oline-7-carboxamide (13a)

Orange solid, yield 40%. ^{1}H NMR (400 MHz, DMSO-d_6) δ 10.83 (s, 1H), 9.01 (t, J = 5.2 Hz, 1H), 8.92 (d, J = 3.0 Hz, 1H), 8.34 (d, J = 8.2 Hz, 1H), 7.99 (d, J = 8.8 Hz, 1H), 7.67–7.63 (m, 1H), 7.62 (d, J = 8.6 Hz, 1H), 7.42 (d, J = 8.8 Hz, 1H), 7.35 (d, J = 8.0 Hz, 1H), 7.22 (s, 1H), 7.08 (t, J = 7.4 Hz, 1H), 6.99 (t, J = 7.3 Hz, 1H), 3.66 (dd, J = 13.4, 6.9 Hz, 2H), 3.03 (t, J = 7.3 Hz, 2H). ^{13}C NMR (126 MHz, DMSO-d_6) δ 168.62, 157.48, 149.58, 139.71, 136.75, 136.45, 131.12, 130.11, 127.68, 125.38, 123.95, 123.27, 121.45, 118.77, 117.35, 112.96, 112.08, 111.89, 40.60, 25.51. HRMS (ESI) m/z calcd for C$_{20}$H$_{17}$N$_3$O$_2$ [M + H]$^+$, 332.1373; found, 332.1354. HPLC purity: 98.9%. Retention time: 5.0 min.

3.1.18 8-hydroxy-N-(2-(5-methoxy-1H-indol-3-yl) ethyl)quinoline-7-carboxamide (13b)

Orange solid, yield 45%. ^{1}H NMR (400 MHz, DMSO-d_6) δ 10.67 (s, 1H), 9.00 (t, J = 5.4 Hz, 1H), 8.92 (dd, J = 4.1, 1.5 Hz, 1H), 8.35 (dd, J = 8.3, 1.4 Hz, 1H), 8.00 (d, J = 8.8 Hz, 1H), 7.65 (dd, J = 8.3, 4.2 Hz, 1H), 7.42 (d, J = 8.8 Hz, 1H), 7.24 (d, J = 8.7 Hz, 1H), 7.18 (d, J = 2.1 Hz, 1H), 7.09 (d, J = 2.2 Hz, 1H), 6.72 (dd, J = 8.7, 2.3 Hz, 1H), 3.66 (dd, J = 13.2, 7.0 Hz, 2H), 3.00 (t, J = 7.3 Hz, 2H). ^{13}C NMR

(126 MHz, DMSO-d_6) δ 168.62, 157.44, 153.48, 149.58, 139.67, 136.47, 131.87, 131.11, 128.03, 125.38, 123.96, 123.93, 117.35, 112.96, 112.53, 111.93, 111.62, 100.58, 55.71, 40.61, 25.48. HRMS (ESI) m/z calcd for $C_{21}H_{19}N_3O_3$ [M + H]$^+$, 362.1466; found, 362.1460. HPLC purity: 97.5%. Retention time: 5.1 min.

3.1.19 N-((1H-indol-3-yl)methyl) -8-hydroxyquinoline-7-carboxamide (13c)

Orange solid, yield 50%. ^{1}H NMR (400 MHz, DMSO-d_6) δ 11.00 (s, 1H), 9.12 (t, J = 5.2 Hz, 1H), 8.90 (dd, J = 4.1, 1.4 Hz, 1H), 8.34 (dd, J = 8.3, 1.4 Hz, 1H), 8.06 (d, J = 8.8 Hz, 1H), 7.70–7.65 (m, 1H), 7.65–7.62 (m, 1H), 7.41 (d, J = 8.8 Hz, 1H), 7.41–7.38 (m, 1H), 7.38–7.36 (m, 1H), 4.75 (d, J = 5.4 Hz, 2H). ^{13}C NMR (126 MHz, DMSO-d_6) δ 167.89, 157.00, 149.47, 139.58, 136.81, 136.51, 131.06, 126.94, 125.77, 124.75, 123.93, 121.70, 119.17, 119.10, 117.36, 113.23, 112.19, 112.01, 35.04. HRMS (ESI) m/z calcd for $C_{19}H_{15}N_3O_2$ [M + H]$^+$, 318.1219; found, 318.1198. HPLC purity: 99.5%. Retention time: 4.7 min.

3.2 Thioflavin T fluorometric detection

Detection of the compounds for disaggregated and inhibitory effects on Cu^{2+} induced Aβ$_{1-42}$ aggregation. Aβ$_{1-42}$ (Sigma-Aldrich A9810, 20 μM) was dissolved in HEPES buffer (pH = 6.6, containing 1% ammonium hydroxide). 10 μL of Aβ$_{1-42}$ was previously incubated with or without Cu^{2+} at 37°C for 3 days to pre-fibrillation. 10 μL of 6b, CQ, and MT (150 μM, in DMSO) were incubated before or after the pre-fibrillation of Aβ$_{1-42}$ at 37°C for 1 day. After incubation, 170 μL of thioflavin T (5 μM, in 50 mM glycine-NaOH buffer) was added to mix well. After incubation for 5 min, the Aβ$_{1-42}$ aggregation was detected by Microplate Reader (HITACHI, F-4700) with excitation/emission at 450/485 nm.

3.2.1 Oxygen radical absorbance capacity (ORAC-FL) assay

The testes compounds and fluorescein (FL) stock solution were diluted with 75 mM phosphate buffer (pH 7.4) to 5 μM and 0.117 μM, respectively (Wang et al., 2018). The solution of Trolox was diluted with 75 mM phosphate buffer to 40, 20, 10, 5, 2.5, and 1.25 μM. The solution of 2,2′-azobis- (amidinopropane) dihydrochloride (AAPH) was prepared to a final concentration of 40 mM. The mixture of the tested compounds (20 μL) and FL (120 μL; 70 nM) was pre-incubated for 10 min at 37°C, 60 μL of the AAPH solution was added. The fluorescence was recorded every minute for 120 min (excitation, 485 nm; emission, 520 nm). The antioxidant curves (fluorescence versus time) were normalized to the curve of the blank. The area under the fluorescence decay curve (AUC) was calculated as the following equation:

$$AUC = 1 + \sum_{i=1}^{i=120} fi/f0$$

Where $f0$ is the initial fluorescence reading at 0 min and fi is the fluorescence reading at time i. The net AUC was calculated by the expression: AUC_{sample}—AUC_{blank}. Regression equations between net AUC and Trolox concentration were calculated. ORAC-FL value of the tested compound expressed as Trolox equivalents.

3.2.2 Inhibition of Aβ$_{1−42}$ aggregation assay

Following the previous literature (Rosini et al., 2008; Wang et al., 2018), Aβ$_{1−42}$ (Sigma-Aldrich) was dissolved in NH_4OH (1% v/v) to get a stock solution, which was aliquoted into small samples and stored at −80°C.

3.2.3 Metal-chelating study

6b and 6c (50 μM) were incubated with $CuSO_4$, $FeSO_4$, $FeCl_3$, or $ZnCl_2$ (50 μM) in buffer (20 mM HEPES, 150 mM NaCl, pH 7.4) for 30 min, and the absorption spectras were recorded at room temperature. For the stoichiometry of the compound–Cu^{2+} complex, a fixed amount of 6b and 6c (50 μM) was mixed with growing amounts of copper ion (0–100 μM), and the difference UV–vis spectra were examined to investigate the ratio of ligand/metal in the complex.

3.2.4 Statistical analysis

Data were presented as mean ± standard deviation (SD) (represented by error bars). All the experiments had three replicates (n = 3). In vivo anti-tumor Student's t-test was used for comparing two groups, and significant differences were indicated by *$p < 0.05$, *$p < 0.01$, ***$p < 0.001$. The statistical analysis was performed with GraphPad Prism 8.0.1.

4 Conclusion

In this study, a series of novel melatonin–hydroxyquinoline hybrids were designed and synthesized, simultaneously targeting anti-oxidation and metal-chelating. Most of the compounds possess good blood-brain barrier permeability and showed significant oxygen radical absorbance capacity and Aβ$_{1−42}$ aggregation inhibition. Among them, 6b and 6c have a good ability to alleviate oxidative stress (Figure 2C) induced by hydrogen peroxide and exhibit metal-chelating properties with the chelation ratio being 2:1. Furthermore, 6b can significantly mitigate metal ion induced Aβ aggregation.

Data availability statement

The datasets presented in this study can be found in online repositories. The names of the repository/repositories and accession number(s) can be found in the article/Supplementary Material.

Author contributions

WW: Writing–original draft, Investigation, Methodology, Validation. TP: Investigation, Methodology, Writing–original draft. RS: Methodology, Writing–original draft, Formal Analysis. MC: Writing–original draft, Data curation. WX: Writing–original draft, Methodology. CX: Writing–original draft, Conceptualization, Funding acquisition, Writing–review and editing. LH: Conceptualization, Supervision, Writing–review and editing.

Funding

Conflict of interest

The authors declare that the research was conducted in the absence of any commercial or financial relationships that could be construed as a potential conflict of interest.

Publisher's note

All claims expressed in this article are solely those of the authors and do not necessarily represent those of their affiliated organizations, or those of the publisher, the editors and the reviewers. Any product that may be evaluated in this article, or claim that may be made by its manufacturer, is not guaranteed or endorsed by the publisher.

Supplementary material

The Supplementary Material for this article can be found online at: https://www.frontiersin.org/articles/10.3389/fchem.2024.1374930/full#supplementary-material

References

Adlard, P. A., Cherny, R. A., Finkelstein, D. I., Gautier, E., Robb, E., Cortes, M., et al. (2008). Rapid restoration of cognition in Alzheimer's transgenic mice with 8-hydroxy quinoline analogs is associated with decreased interstitial Aβ. *Neuron* 59, 43–55. doi:10.1016/j.neuron.2008.06.018

Author Anonymous (2023). Alzheimer's disease facts and figures. *Alzheimers Dement.* 19, 1598–1695. doi:10.1002/alz.12328

Babaei, E., Kucukkilinc, T. T., Jalili-Baleh, L., Nadri, H., Oz, E., Forootanfar, H., et al. (2022). Novel coumarin-pyridine hybrids as potent multi-target directed ligands aiming at symptoms of Alzheimer's disease. *Front. Chem.* 10, 895483. doi:10.3389/fchem.2022.895483

Cerejeira, J., Lagarto, L., and Mukaetova-Ladinska, E. B. (2012). Behavioral and psychological symptoms of dementia. *Front. Neurol.* 3, 73. doi:10.3389/fneur.2012.00073

Di, L., Kerns, E. H., Fan, K., McConnell, O. J., and Carter, G. T. (2003). High throughput artificial membrane permeability assay for blood-brain barrier. *Eur. J. Med. Chem.* 38, 223–232. doi:10.1016/s0223-5234(03)00012-6

Dowling, G. A., Burr, R. L., Van Someren, E. J., Hubbard, E. M., Luxenberg, J. S., Mastick, J., et al. (2008). Melatonin and bright-light treatment for rest-activity disruption in institutionalized patients with Alzheimer's disease. *J. Am. Geriatr. Soc.* 56, 239–246. doi:10.1111/j.1532-5415.2007.01543.x

Faux, N. G., Ritchie, C. W., Gunn, A., Rembach, A., Tsatsanis, A., Bedo, J., et al. (2010). PBT2 rapidly improves cognition in Alzheimer's disease: additional phase II analyses. *J. Alzheimers. Dis.* 20, 509–516. doi:10.3233/jad-2010-1390

Geng, J., Li, M., Wu, L., Ren, J., and Qu, X. (2012). Liberation of copper from amyloid plaques: making a risk factor useful for Alzheimer's disease treatment. *J. Med. Chem.* 55, 9146–9155. doi:10.1021/jm3003813

He, L., Du, J. J., Zhou, J. J., Chen, M. T., Luo, L., Li, B. Q., et al. (2022). Synthesis of melatonin derivatives and the neuroprotective effects on Parkinson's disease models of *Caenorhabditis elegans*. *Front. Chem.* 10, 918116. doi:10.3389/fchem.2022.918116

Hu, J., Pan, T., An, B., Li, Z., Li, X., and Huang, L. (2019). Synthesis and evaluation of clioquinol-rolipram/roflumilast hybrids as multitarget-directed ligands for the treatment of Alzheimer's disease. *Eur. J. Med. Chem.* 163, 512–526. doi:10.1016/j.ejmech.2018.12.013

Lu, C., Guo, Y., Yan, J., Luo, Z., Luo, H. B., Yan, M., et al. (2013). Design, synthesis, and evaluation of multitarget-directed resveratrol derivatives for the treatment of Alzheimer's disease. *J. Med. Chem.* 56, 5843–5859. doi:10.1021/jm400567s

Marcinkowska, M., Bucki, A., Sniecikowska, J., Zagórska, A., Fajkis-Zajączkowska, N., Siwek, A., et al. (2021). Multifunctional arylsulfone and arylsulfonamide-based ligands with prominent mood-modulating activity and benign safety profile, targeting neuropsychiatric symptoms of dementia. *J. Med. Chem.* 64, 12603–12629. doi:10.1021/acs.jmedchem.1c00497

Reiter, R. J., Mayo, J. C., Tan, D. X., Sainz, R. M., Alatorre-Jimenez, M., and Qin, L. L. (2016). Melatonin as an antioxidant: under promises but over delivers. *J. Pineal Res.* 61, 253–278. doi:10.1111/jpi.12360

Rosini, M., Simoni, E., Bartolini, M., Cavalli, A., Ceccarini, L., Pascu, N., et al. (2008). Inhibition of acetylcholinesterase, β-amyloid aggregation, and nmda receptors in Alzheimer's disease: a promising direction for the multi-target-directed ligands gold rush. *J. Med. Chem.* 51, 4381–4384. doi:10.1021/jm800577j

Rossi, M., Freschi, M., de Camargo Nascente, L., Salerno, A., de Melo Viana Teixeira, S., Nachon, F., et al. (2021). Sustainable drug discovery of multi-target-directed ligands for Alzheimer's disease. *J. Med. Chem.* 64, 4972–4990. doi:10.1021/acs.jmedchem.1c00048

Scheltens, P., De Strooper, B., Kivipelto, M., Holstege, H., Chételat, G., Teunissen, C. E., et al. (2021). Alzheimer's disease. *Lancet* 397, 1577–1590. doi:10.1016/s0140-6736(20)32205-4

Somalo-Barranco, G., Serra, C., Lyons, D., Piggins, H. D., Jockers, R., and Llebaria, A. (2022). Design and validation of the first family of photo-activatable ligands for melatonin receptors. *J. Med. Chem.* 65, 11229–11240. doi:10.1021/acs.jmedchem.2c00717

Turgutalp, B., Bhattarai, P., Ercetin, T., Luise, C., Reis, R., Gurdal, E. E., et al. (2022). Discovery of potent cholinesterase inhibition-based multi-target-directed lead compounds for synaptoprotection in Alzheimer's disease. *J. Med. Chem.* 65, 12292–12318. doi:10.1021/acs.jmedchem.2c01003

Wang, Z., Hu, J., Yang, X., Feng, X., Li, X., Huang, L., et al. (2018). Design, synthesis, and evaluation of orally bioavailable quinoline–indole derivatives as innovative multitarget-directed ligands: promotion of cell proliferation in the adult murine Hippocampus for the treatment of Alzheimer's disease. *J. Med. Chem.* 61, 1871–1894. doi:10.1021/acs.jmedchem.7b01417

Wang, Z., Wang, Y., Li, W., Mao, F., Sun, Y., Huang, L., et al. (2014). Design, synthesis, and evaluation of multitarget-directed selenium-containing clioquinol derivatives for the treatment of Alzheimer's disease. *ACS Chem. Neurosci.* 5, 952–962. doi:10.1021/cn500119g

Wang, Z., Wang, Y., Wang, B., Li, W., Huang, L., and Li, X. (2015). Design, synthesis, and evaluation of orally available clioquinol-moracin M hybrids as multitarget-directed ligands for cognitive improvement in a rat model of neurodegeneration in Alzheimer's disease. *J. Med. Chem.* 58, 8616–8637. doi:10.1021/acs.jmedchem.5b01222

Xu, C., Yang, H., Xiao, Z., Zhang, T., Guan, Z., Chen, J., et al. (2021). Reduction-responsive dehydroepiandrosterone prodrug nanoparticles loaded with camptothecin for cancer therapy by enhancing oxidation therapy and cell replication inhibition. *Int. J. Pharm.* 603, 120671. doi:10.1016/j.ijpharm.2021.120671